Environments of the Four Tryptophans in the Extracellular Domain of Human Tissue Factor: Comparison of Results from Absorption and Fluorescence Difference Spectra of Tryptophan Replacement Mutants with the Crystal Structure of the Wild-Type Protein

C. A. Hasselbacher,* E. Rusinova,* E. Waxman,* R. Rusinova,* R. A. Kohanski,* W. Lam,‡ A. Guha,‡ J. Du,§ T. C. Lin,§ I. Polikarpov,¶ C. W. G. Boys,¶ Y. Nemerson,*‡ W. H. Konigsberg,§ and J. B. A. Ross*

Departments of *Biochemistry and ‡Medicine, Mount Sinai School of Medicine, New York, New York 10029, and §Department of Biochemistry, Yale University, New Haven, Connecticut 06510 USA; and ¶Department of Biochemistry, The Medical School, Edinburgh EH8 9XD, United Kingdom

ABSTRACT The local environments of the four tryptophan residues of the extracellular domain of human tissue factor (sTF) were assessed from difference absorption and fluorescence spectra. The difference spectra were derived by subtracting spectra from single Trp-to-Phe or Trp-to-Tyr replacement mutants from the corresponding spectrum of the wild-type protein. Each of the mutants was capable of enhancing the proteolytic activity of factor VIIa showing that the mutations did not introduce major structural changes, although the mutants were more susceptible to denaturation by guanidinium chloride. The difference spectra indicate that the Trp residues are buried to different extents within the protein matrix. This evaluation was compared with the x-ray crystal structure of sTF. There is excellent agreement between predictions from the difference spectra and the environments of the Trp residues observed in the x-ray crystal structure, demonstrating that difference absorption and particularly fluorescence spectra derived from functional single-Trp replacement mutants can be used to obtain information about the local environments of individual Trp residues in multi-tryptophan proteins.

INTRODUCTION

The absorbance and fluorescence characteristics of tryptophan residues provide direct information about the chemical nature of the local environment surrounding the indole side chain. Specifically, the sensitivity of the fluorescence spectrum, emission intensity, lifetime, and anisotropy to the local environment makes Trp spectra invaluable tools for probing conformational change. An extensive literature has been established recently in which intrinsic fluorescence is used to analyze Trp environments of single-Trp proteins that occur naturally or are created by recombinant genetic techniques. Because of the obvious difficulties in resolving fluorescence signals from multiple, similar fluorophores, it is difficult to obtain information that is as detailed from the more commonly occurring proteins that contain several Trp residues.

One approach to simplify spectral analysis is to generate amino acid replacements of all but one Trp residue with the anticipation that the resulting absorption and fluorescence will be characteristic of that single Trp residue as it behaved in the original wild-type protein. Not surprisingly, however, simultaneous replacement of several residues often results in failure of protein expression or in expression of mutant proteins that are nonfunctional or conformationally nonrepresentative of the parent molecule. To minimize these perturbations, we have taken a more conservative approach in which individual Trp residues in a multi-Trp protein are replaced one at a time with either Phe or Tyr, systematically generating a panel of mutants that have one fewer Trp than the parent protein. Then the absorbance and fluorescence spectra of the eliminated Trp are obtained by the difference between the mutant and wild-type protein spectra. This latter strategy is based on the assumption that replacement of a single indole group with another aromatic group is less likely to introduce a major perturbation of the protein's structure.

We have applied the strategy of single-Trp replacement difference spectroscopy to an analysis of the Trp environments of the extracellular domain of human tissue factor (TF). Soluble TF (sTF) contains four Trp residues, several of which are in functionally important regions (Rehemtulla et al., 1992; Ruf et al., 1992a,b, 1994). The full-length parent protein is a 263-residue, membrane-bound glycoprotein that has an essential role in the initiation of blood coagulation (Bach, 1988; Nemerson, 1988; Edgington et al., 1991). In addition to the extracellular domain (residues 1–219), TF includes a single transmembrane domain (residues 220–242) followed by a short cytoplasmic tail (residues 243–263) (Spicer et al., 1987). After tissue damage, the extracellular domain of TF binds to coagulation factors VII and VIIa, both of which circulate in the blood. Formation of the complex with TF is essential for the proteolytic activity of VIIa, and this procoagulant proteolytic activity is the best index of TF function. The truncated form of TF, sTF, prepared in our laboratory contains the first 218 residues of the extracellular domain, and it forms a high affinity complex with VIIa (Waxman et al., 1992, 1993a). Although

Received for publication 23 January 1995 and in final form 4 April 1995.

Address reprint requests to Dr. J. B. Alexander Ross, Department of Biochemistry, Mount Sinai School of Medicine, Box 1020, One Gustave L. Levy Place, New York, NY 10029-0574. Tel. 212-241-5569; Fax: 212-996-7214; E-mail: sross@smtplink.mssm.edu.

0006-3495/95/07/20/10 $2.00

sTF lacks the transmembrane and cytoplasmic portions of the native molecule, in the presence of phospholipids it retains procoagulant activity (Waxman et al., 1992; Neuenschwander and Morrissey, 1992; Fiore et al., 1994).

To carry out a spectroscopic analysis of the local environments of the four Trp residues in sTF, we prepared a set of Trp-to-Phe or Trp-to-Tyr single replacement mutants of sTF. To evaluate perturbations of protein structure caused by mutation, stability against denaturation in guanidinium chloride (Gdm·Cl) was measured. To evaluate function, mutant sTF:VIIa binding affinities and proteolytic activities were measured. The features of the local environments of the Trp residues were then deduced from the difference spectra of the mutants versus the wild-type protein. Finally, to assess the validity of this approach, the results of the spectroscopic analysis were compared with information about the local environments of the individual Trp residues obtained from the x-ray crystal structure of the 219-residue extracellular domain of human TF determined by Harlos et al. (1994).

MATERIALS AND METHODS

Reagents

Human recombinant VIIa was purchased from NOVO Nordisk (Denmark), and factor X was purified from human plasma by methods of Miletich et al. (1981) and Broze and Majerus (1980). The concentration of X was determined by using an $A^{1\%(1\ cm)}$ of 11.6 at 280 nm (Di Scipio et al., 1977). Purified factor Xa was prepared by Dr. H. Andree. The chromogenic substrate for Xa, Ile-Pro-Arg-*p*-nitroanilide (IPR-*p*NA) was synthesized by Dr. G. Schwartz. VII-deficient plasma was prepared in our laboratory by using an immunoadsorption anti-VII Affigel-10 column to remove factor VII. Thrombofax was purchased from Ortho Diagnostic System (Raritan, NJ). 1,2-Dioleoyl-*sn*-glycero-3-phosphatidylserine (DOPS) and 1,2-dioleoyl-*sn*-glycero-3-phosphatidylcholine (DOPC) were obtained from Avanti Polar Lipids (Alabaster, AL). Guanidinium chloride was purchased from Heico Chemicals (Delaware Water Gap, PA). Endoproteinase Lys-C was obtained from Boehringer Mannheim (Indianapolis, IN). Restriction enzymes were from New England Biolabs (Beverly, MA).

Mutation of the tryptophan residues in sTF

Construction of the vector for bacterial expression of sTF, p6TF219, is described elsewhere (Waxman et al., 1992; W. H. Konigsberg, J. B. A. Ross, A. Guha, S. V. Thiruvikraman, C. Fang, and Y. Nemerson, submitted for publication). The following oligonucleotides were used for Trp mutations in the expression vector p6TF219; the triplet base changes coding for Phe or Tyr are in lowercase, the new restriction cleavage sites are underlined, and the corresponding restriction enzyme is given in parentheses after each sequence: (1) Trp-14 to Phe-14 (W14F), 5′-GGCAGCATATAATTTAACTttt AAATCAACTAATTTC-3′ (*Dra*I); (2) Trp-45 to Phe-45 (W45F), 5′-CAAATAAGCACTAAGTCCGGAGATtcAAAAGCAAATGCTTT-3′ (*Bst*BI); (3) Trp-158 to Phe-158 (W158F), 5′-CTTAATTTATACACTTTATTATtttAAATCTTCAAGTTCAGG-3′ (*Dra*I); and (4) Trp-25 to Tyr-25 (W25Y), 5′-CTAATTTCAAGACAATTCTCGAGtacGAACCCAAACCCGTC-3′ (*Xho*I).

Expression, purification, and confirmation of sTF and mutants

The plasmids, transformed into *Escherichia coli* strain BL-21 (DE-3), were grown in a 2-L Virtis fermenter at 37°C in DE-3 media (40 mM Na_2HPO_4, 20 mM KH_2PO_4, 10 mM NaCl, 0.1 M NH_4Cl, glycerol (25 g/L), and tryptone (10 g/L)), with added oxygen and maintenance of pH at 7.4, for approximately 6 h. After induction with 1 mM (final concentration) isopropyl-D-thiogalactopyranoside, the cells were allowed to grow for 16 h at room temperature. Protein from the media was purified and characterized as described (Waxman et al., 1992). The Trp mutations were checked by high pressure liquid chromatography peptide mapping after digestion with Endolys-C. Peptides containing the mutated residues were identified on the basis of their absorption spectra obtained on-line during the high pressure liquid chromatography and confirmed by amino acid sequence analyses. Criteria for protein purity was by Coomassie-stained polyacrylamide gel electrophoresis and by linear combination of spectra analysis of the absorbance spectra (Waxman et al., 1993b).

Using the fermentation procedure described above, under optimal circumstances we have been able to produce >50 mg/L media of purified wild-type sTF. Typical yields during the course of these experiments were ~15 mg/L media, which represents a significant improvement over protein expression by culture in shaker flasks. Also, it facilitates protein purification because most of the protein in the culture media is sTF. Yields of the mutants were variable. The yield of W158F was equivalent to sTF, whereas that of W45F was approximately one-half that of sTF. The yield of W14F was an order of magnitude less than that of sTF (~2 mg/L media), and using both fermenter and shaker flask culture protocols we were unable to express sufficient W25F (Trp-25 to Phe-25) for purification. However, W25Y was expressed in sufficient amounts (~2 mg/L media) for characterization by absorption and fluorescence spectroscopy.

Cofactor activity assay of sTF and mutants

We previously have shown that the association of sTF with VIIa yields a 1:1 stoichiometric complex with an equilibrium dissociation constant of ~1 nM (Waxman et al., 1992). In the following, we refer to both sTF and the mutants as cofactor. To compare the apparent dissociation constants and relative catalytic efficiencies of sTF and sTF mutants with VIIa, we titrated VIIa over a range of cofactor concentrations from 0 to 2 μM and monitored the cofactor:enzyme complex by its ability to convert X to Xa. An automated robotic system, developed by our laboratory, was used to perform this assay. Briefly, cofactor was added to a solution of VIIa (1 nM), X (100 nM), and Ca^{2+} (5 mM); (final concentrations) in HEPES-buffered saline with bovine serum albumin (BSA), containing 10 mM HEPES, 0.14 M NaCl, 1 mg/ml BSA, pH 7.5. After 5 min equilibration of the 285-μL sample at 25°C, conversion of X to Xa was initiated by addition of 15 μL of 0.2 mM DOPS/DOPC phospholipid vesicles (30/70 w/w; final phospholipid concentration of 10 μM). At 30-s intervals, 20-μL aliquots were withdrawn and transferred to microtiter wells that contained 125 μL of 50 mM EDTA in HEPES buffered saline with BSA to terminate conversion of X to Xa. Then the chromogenic substrate IPR-*p*NA was added to a final concentration of 1.5 mM. The amount of Xa produced at each time point was determined by measuring the rate of hydrolysis of IPR-*p*NA; the slope of the initial absorbance increase at 405 nm versus time, calculated by linear regression, was proportional to the Xa concentration. The amount of Xa produced by the different complexes was determined by comparison to a standard curve of IPR-*p*NA hydrolysis at known concentrations of purified Xa.

A particular mutation can change the binding of cofactor to VIIa. It can also change the enzymatic activity of the complex. These effects are described by the apparent equilibrium dissociation constant for the cofactor:VIIa complex and the maximum velocity for conversion of X to Xa, respectively. (The underlying assumption is that X binding is essentially equivalent for all cofactor:VIIa complexes and therefore does not affect their apparent dissociation constants. We point out that this assumption is implicit in all studies using X activation to evaluate TF:VIIa interactions.) An apparent dissociation constant for each cofactor:VIIa complex was determined by measuring VIIa activity at increasing concentrations of cofactor and at a saturating concentration of the substrate X. The VIIa concentration was 1 nM, near that of the dissociation constant for the

complex of unmodified sTF and VIIa, previously determined by pressure perturbation (Waxman et al., 1992). In this situation, the observed velocity, V_{obs}, as a function of cofactor concentration, reflects directly the concentration of cofactor:VIIa complex:

$$V_{obs} = [\text{cofactor:VIIa}]k_{cat}\,. \quad (1)$$

A maximum velocity, $V_{max\ cofactor}$, is achieved in the titration when VIIa is saturated with cofactor, i.e., sTF. This leads to an expression that defines the equilibrium concentration of the VIIa:cofactor complexes in terms of the observables, such that

$$[\text{cofactor:VIIa}] = \left[\frac{V_{obs}}{V_{max\ cofactor}}\right][\text{VIIa}_o]\,, \quad (2)$$

where $[\text{VIIa}_o]$ is the total VIIa concentration. Apparent dissociation constants, K_d, were obtained by fitting the titration data by least squares using the appropriate root of the quadratic equation

$$[\text{cofactor:VIIa}]^2 - [\text{cofactor:VIIa}](K_d + [\text{VIIa}_o] + [\text{cofactor}_o]) + [\text{VIIa}_o][\text{cofactor}_o] = 0\,, \quad (3)$$

where $[\text{cofactor}_o]$ is the total cofactor concentration at each point in the titration. Comparison of $V_{max\ cofactor}$ of each mutant to $V_{max\ sTF}$ reflects directly the catalytic efficiencies of the complexes. These titrations do not reveal potential changes in K_m of the complex for substrate X because the substrate concentration was both constant and saturating; thus changes in k_{cat} are determined simply, without elaborate kinetic analysis.

Ultraviolet absorption, circular dichroism, and fluorescence spectroscopy

Unless otherwise noted, spectroscopic measurements were made by using 0.1 M NaCl, 0.05 M Tris, pH 7.5, buffer. Absorption spectra were measured at room temperature with a dual-beam Hitachi U-3210 spectrophotometer. Molar extinction coefficients were determined for sTF and mutants by diluting and denaturing an aliquot of each sample stock in 6 M Gdm·Cl and measuring the spectra. The concentration of denatured protein was then calculated from knowledge of the protein's Trp and Tyr content and the Beer-Lambert law, by using a value of 5500 $M^{-1}cm^{-1}$ for the 280-nm extinction coefficient of Trp (Wetlaufer, 1962) and by using the relative, scaled 280-nm extinction coefficient of Tyr obtained from Trp- and Tyr-containing peptides in 6 M Gdm·Cl as described previously (Waxman et al., 1993b). The dilutions then provided the appropriate factors for calculating the scaled molar extinctions and the concentrations of the native proteins.

Unfolding as a function of Gdm·Cl concentration was used to assess the structural stabilities of the mutants relative to sTF at pH 7.5 with either 50 mM Tris (fluorescence) or 5 mM phosphate (circular dichroism (CD)) at 24°C. To eliminate kinetic contributions as a result of the unfolding process, the solutions were equilibrated overnight before measurement. CD spectra of samples in 0.2-cm-path-length cells were obtained by using a Jasco J-500A circular dichroism spectrophotometer. The mean residue ellipticity was calculated by using a molecular weight of 24,672, based on the amino acid composition of sTF. Steady-state fluorescence emission spectra (8-nm excitation and emission bandpasses) were obtained with an SLM Aminco SPF 500C spectrofluorometer or an SLM 4800 spectrofluorometer modified in our laboratory for photon counting. To avoid emission intensity artifacts caused by molecular motions that occur during the lifetime of the excited state, magic angle polarization conditions were used for all fluorescence measurements (Badea and Brand, 1979). To minimize the contribution of Tyr residues to emission spectra, 295-nm excitation was used, except where indicated.

Fluorescence quenching by KI at high ionic strengths (0.5-0.6 M) was used to assess solvent accessibility of emissive Trp residues. The average solvent accessibility of the fluorescent Trp residues was characterized in terms of the apparent Stern-Volmer constant, K_{SV}, calculated from the equation

$$F_o/F = 1 + K_{SV}[Q]\,, \quad (4)$$

where F_o is the fluorescence intensity in the absence of quencher, F is the fluorescence intensity in the presence of quencher, and [Q] is the quencher concentration (see Lakowicz, 1983). For the case for which it is known that the fluorescence is caused by a single emitter with multi-exponential intensity decay kinetics and there is no ground-state quenching interaction introduced by the quencher (see below), the observed K_{SV} is the product of the bimolecular collisional quenching constant, k_q, and the mean (intensity average) fluorescence lifetime of the emitter in the absence of quencher, $\langle\tau_o\rangle$, is defined by the equation

$$\langle\tau_o\rangle = \frac{\sum_{i=1}^{n}\alpha_i\tau_i^2}{\sum_{i=1}^{n}\alpha_i\tau_i}\,, \quad (5)$$

where α_i is the amplitude and τ_i is the lifetime of the ith emitting component (see Laws and Contino, 1992; Eftink, 1991). Mean lifetimes were obtained for mutants identified as single Trp emitters by the time-correlated single-photon counting method (see Hasselbacher et al., 1991) at a resolution of 22.3 ps per data point distributed over 2000 points.

Quenching interactions are operationally defined as dynamic or static, according to the kinetic signature of the fluorescence intensity decay compared with the steady-state fluorescence quantum yield. Dynamic quenching reflects an interaction that occurs during the lifetime of the excited state of a fluorophore. Static quenching indicates that, while in the ground state, some fraction of the fluorophores is involved in an interaction that causes that fraction to be nonemissive after excitation by a photon. Although both mechanisms result in a reduction of the steady-state fluorescence intensity, only dynamic quenching results in a reduction of the fluorescence lifetime. For a more detailed discussion, see Lakowicz (1983).

RESULTS AND DISCUSSION

Effects of single Trp replacements in sTF on cofactor activation of VIIa

We compared the cofactor activities of sTF and the Trp mutants as described in Materials and Methods. In these experiments, k_{cat} for the sTF:VIIa complex was 4 min^{-1}, which is in the range that we observed previously (Waxman et al., 1992). Under the assay conditions, the catalytic efficiency as a function of cofactor concentration reflects the degree of saturation of VIIa by cofactor. This yields apparent dissociation constants, which are listed in Table 1. For mutant cofactor concentrations at which VIIa is saturated, we obtain a direct measure of the catalytic efficiencies of the cofactor:VIIa complexes, which are also listed in Table 1. Mutant W14F is comparable with sTF in both binding and conferring catalytic activity to VIIa. The binding affinity between W158F and VIIa also is in the 2 nM range, and the maximal catalytic activity is approximately one-half that of the sTF:VIIa complex. W25Y binding to VIIa is approximately one-fourth that of sTF, but the complex has nearly the same activity as that observed with sTF. Although W45F displays the weakest association with VIIa, approximately an order of magnitude weaker than sTF, the com-

TABLE 1 Apparent equilibrium dissociation constants and relative catalytic rate constants for the mutant and wild-type sTF complexes with VIIa

Cofactor	K_d (nM)	k_{cat} (min^{-1})
sTF	2	4.0
W14F	2	4.0
W25Y	7	3.2
W45F	20	2.4
W158F	2	2.4

Apparent equilibrium dissociation constants (estimated uncertainty, $K_d \div 2$ to $K_d \times 2$) and relative catalytic efficiencies (estimated uncertainty, ±20%) of the cofactor: VIIa complexes at 25°C measured by chromogenic assay as described in Materials and Methods.

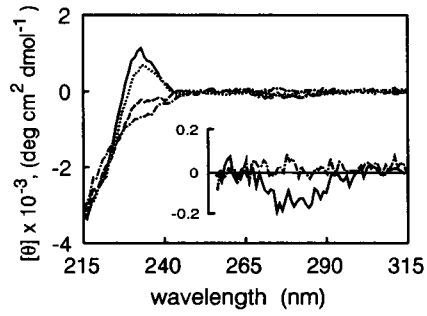

FIGURE 1 The change in the CD spectra of sTF as a function of Gdm·Cl concentration: –, 0 M; ····, 1.25 M; ----, 1.5 M; ---, 2.7 M.

plex still has approximately one-half the catalytic activity as that observed with sTF. The binding and activity of W45Y is identical to W45F (data not shown).

The reduced affinities of W25Y and W45F for VIIa indicate that these residues themselves are either involved in interaction with VIIa or that replacement of the indole ring with the smaller phenol ring or phenyl ring alters the packing constraints of other surface residues that form contacts with VIIa. Nevertheless, once formed, the cofactor:VIIa complexes are all functional. As the essential catalytic efficiency of VIIa results from binding of its cofactor, the twofold or smaller differences in catalytic efficiencies observed here suggest that when the Trp mutants are bound to VIIa they have structures that are very similar to that of the wild-type protein.

Stabilities of sTF and mutant proteins

As pointed out by Eftink (1994), Trp located at different locations within a protein will not necessarily give identical reports about the protein unfolding process as the local environments of each Trp may not be equally resistant to denaturation. As described below, the fluorescence emission of sTF, W14F, W25Y, and W158F is caused mainly by Trp-45 and therefore the initial changes in the emission spectra of these proteins that result from unfolding mainly report on the stability of the environment of Trp-45. Also as described below, the initial change in the fluorescence spectrum of W45F reports mainly on the stability of the local environment of Trp-14, as that is the dominant emitter in this mutant. Therefore, CD, which measures global changes in secondary structure, was used also to evaluate stability as well as refolding.

An example of the effect of Gdm·Cl upon the CD spectrum is shown for sTF in Fig. 1. It should be noted that the ultraviolet CD of native sTF for the region between 210 and 250 nm is similar to that reported previously by Ruf and Edgington (1991), who interpreted the CD in terms of a secondary structure composed of 62–65% β-strand, 23–25% random coil, and 11–13% β-turn. The characteristic feature in the region between 210 and 250 nm is a prominent band with positive ellipticity centered near 232 nm. There is also a weaker negative band in the region near 280 nm, indicated by the inset in Fig. 1, for which the absorbance is dominated by the aromatic rings of Tyr and Trp. Both features disappear upon denaturation in Gdm·Cl and, within experimental error, the changes in the CD spectra are consistent with the changes in the fluorescence spectra. Upon removal of Gdm·Cl by dialysis, the native CD spectrum is recovered, indicating that unfolding of sTF in Gdm·Cl is reversible.

Whereas the emission intensity of W45F increases upon denaturation in Gdm·Cl (Fig. 2*A*), the emission intensities of the other proteins, including W14F, decrease (Fig. 2*B*; shown for sTF). This behavior indicates that the different Trp residues have different quantum yields in the native state. Nevertheless, the centers of gravity of the fluorescence emission spectra of sTF and all the mutants shift to the red upon denaturation in Gdm·Cl, consistent with exposure of the Trp residues to solvent. At approximately 2 M Gdm·Cl and with 295-nm excitation, the emission maxima of all of the proteins are coincident with that of *N*-acetyltryptophanamide (NATA) under the same conditions. As shown in Fig. 3, one-half of the maximal shift in the fluorescence spectrum of sTF occurs at ~1.5 M Gdm·Cl. The half-maximal shift in the spectra of the mutants occurs between 1.1 and 1.2 M Gdm·Cl.

Each of the mutants exhibit reduced stabilities compared with sTF, indicating that each of the Trp indole groups are involved in intramolecular interactions that help to stabilize the protein structure. The emission shifts and changes in the

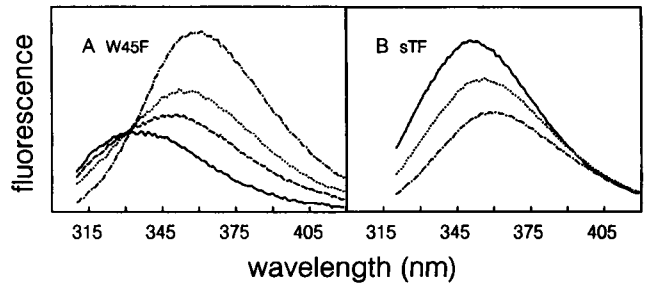

FIGURE 2 Fluorescence emission spectra as a function of Gdm·Cl concentration of W45F mutant (*A*) and sTF (*B*). (*A*) –, 0 M; ----, 1.1 M; ····, 1.2 M; ---, 3.0 M. (*B*) –, 0 M; ····, 1.5 M; ---, 3.0 M.

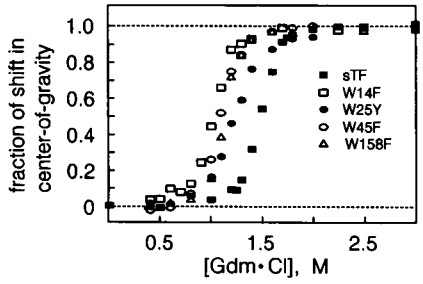

FIGURE 3 Dependence on Gdm·Cl concentration in center of gravity shifts of the emission spectra of sTF (■), W14F (□), W25Y (●), W45F (○), and W158F (△).

fluorescence intensities of sTF and the four mutants in Gdm·Cl reflect the loss in the denatured state of specific indole ring interactions in each Trp environment. Also, it should be noted that the emission spectra of W45F obtained at different Gdm·Cl concentrations exhibit an isoemissive point (Fig. 2*A*). This is consistent with a two-state process for the unfolding of W45F. Moreover, the denaturation progress curves of W14F and W158F are essentially indistinguishable from that of W45F (Fig. 3), which suggests that their unfolding proceeds in the same fashion and that their three Trp residues report identically the same pathway of unfolding. In contrast, the denaturation curve of W25Y is intermediate between those for the other mutants and sTF. Compared with the other proteins, denaturation of W25Y proceeds over a broader range of Gdm·Cl concentrations, suggesting that unfolding of this mutant is different and that one or more of the three remaining Trp residues is reporting a change in unfolding pathway resulting from replacement of Trp-25.

Resolved absorbance spectra of the individual tryptophan residues in sTF

The absorption spectrum of each protein was obtained for the wavelength region 260–340 nm, as described in Materials and Methods. The individual spectrum of each Trp was then calculated for the wavelength range 270–320 nm (to exclude significant absorption from Phe residues) by subtraction of each mutant protein spectrum (three Trp residues) from that of sTF (four Trp residues). It should be noted that three of the mutants, W14F, W45F, and W158F, and sTF itself contain the same number of Tyr residues. In this way, we resolved the spectra of Trp-14, Trp-45, and Trp-158 (Fig. 4). However, as described in Materials and Methods, W25F did not express well. Therefore, calculation of the spectrum of Trp-25 required the use of mutant W25Y. This situation made it necessary to account for an additional Tyr residue in the mutant.

Because the absorbance of this Tyr residue in the folded protein could not be resolved directly, the assumption was made that its absorption could be adequately represented by the number average absorption of all 12 Tyr residues in the mutant. The total Tyr absorbance of

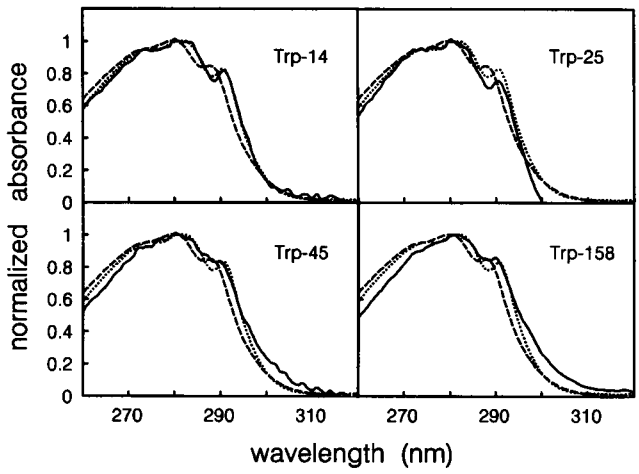

FIGURE 4 Comparison of normalized absorbance spectra of the four Trp in sTF (–) with that of NATA in aqueous buffer (- - -) and in dioxane (····).

W25Y was obtained by subtracting the absorption contributions of Trp-14, Trp-45, and Trp-158, calculated from the other three mutants, from the spectrum of W25Y. The difference spectrum obtained by this procedure had an absorption maximum at 278 nm, characteristic of Tyr, and showed no obvious contribution from Trp. This result indicates that the resolved Trp spectra obtained from the other three mutants represent accurate estimates of the absorption contributions of Trp-14, Trp-45, and Trp-158 in W25Y. The number average (1/12) of the calculated Tyr spectrum was subtracted from that of W25Y and the resulting spectrum was subtracted from that of sTF, generating the spectrum attributed to Trp-25, shown in Fig. 4. It should be noted that the difference spectrum of trp-25 in Fig. 4 is negative in the region >300 nm and returns to zero at 310 nm. The negative deflection, which represents 10% of the total normalized Trp difference spectrum, probably reflects error from using the number average Tyr absorbance to estimate the absorbance for the Tyr residue introduced at position 25. This is no surprise as it is known that the absorbance of Tyr residues depend upon the local environments (Wetlaufer, 1962; Ross et al., 1992a). However, as the negative base line deflection could be eliminated by rescaling the calculated Tyr absorption, and this procedure does not affect significantly either the positions or resolution of the Trp-25 difference spectrum, we conclude that the base line error does not alter in any substantial way the conclusions drawn from the difference spectrum generated for Trp-25.

The individual Trp absorption spectra in Fig. 4 are compared with those of NATA in aqueous buffer, which models a protein-bound Trp exposed to polar medium, and NATA in dioxane, which models a Trp residue buried in the protein interior. All four difference spectra are red-shifted compared with NATA in aqueous buffer.

This suggests that the four Trp in the native protein are not fully exposed to the aqueous solvent. In addition, the spectra of Trp-14 and Trp-25 show greater resolution of the characteristic vibronic band of the ^1L_b electronic transition of indole that occurs near 290 nm (Strickland et al., 1971; Valeur and Weber, 1977). Greater resolution of the electronic transitions, as a result of narrower vibrational bands, generally reflects a smaller distribution of interactions with the neighboring chemical groups in the local environment of a Trp residue (Ross et al., 1980). This could result from greater packing restrictions for the indole rings of Trp-14 and Trp-25 compared with those of Trp-45 or Trp-158.

Fluorescence emission spectra of the Trp residues in sTF

With excitation at 295 nm, the intensities and shapes of the steady-state fluorescence spectra of W25Y and W158F are identical within experimental error to that of sTF, shown in Fig. 5*A*. This indicates that Trp-25 and Trp-158 do not fluoresce. By contrast, the emission intensities of both W14F and W45F are weaker than that of sTF; according to the integrated spectra, W14F accounts for 73 ± 3% and W45F accounts for 23 ± 1% of the total steady-state fluorescence yield of sTF. Thus, the fluorescence emission of sTF can be accounted for by the combined yields of W14F and W45F, indicating that Trp-14 and Trp-45 are the dominant emitters in sTF, as shown in Fig. 5*A*. This result also indicates that the emission spectrum of W45F is due to Trp-14 and that of W14F is due to Trp-45. Because Rayleigh scattering caused by the protein distorts the high energy side of the emission spectra, the spectra are not accurately representative of these two Trp residues. Assuming that the Rayleigh scattering contributions of the mutant and wild-type proteins are identical, more accurate representations can be obtained by subtraction of the mutant spectra from that of the wild-type protein. Based on the relative quantum yields of W14F, W45F, and sTF, the difference fluorescence spectra from W14F and W45F are expected to correlate, respectively, with the resolved emission contributions from Trp-14 and Trp-45. These assigned difference spectra are shown in Fig. 5*B*. Accordingly, the emission spectrum of Trp-14 closely resembles that of NATA in dioxane, and the spectra of both Trp-14 and Trp-45 are blue-shifted compared with that of NATA in neutral pH aqueous buffer. These features of the fluorescence difference spectra indicate that neither residue side chain is fully exposed to the aqueous solvent, consistent with the absorption difference spectra.

Solvent accessibility of the emitting Trp residues of sTF and the mutants was further assessed by quenching of the fluorescence emission. As expected from the close similarity of the fluorescence emission spectra and intensities of sTF, W25Y, and W158F, the fluorescence quenching behaviors of these three proteins were similar. This is consistent with the conclusion that Trp-25 and Trp-158 have insignificant fluorescence yields compared with Trp-14 and Trp-45. The quenching data yielded essentially linear plots with apparent K_{SV} values near 1.8 M^{-1}; see Eq. 4. By contrast, W45F showed significantly less quenching with a K_{SV} value of ~0.2 M^{-1}, and W14F exhibited more quenching with a K_{SV} value of 2.4 M^{-1}. On the basis that the main emitter in W45F is Trp-14 and the main emitter in W14F is Trp-45, the relative exposures of these two Trp residues can be compared directly in terms of their bimolecular quenching constants (k_q). From mean lifetimes of 2.2 ns for W45F and 5.9 ns for W14F, the calculated k_q values are 9×10^7 M^{-1} s^{-1} for Trp-14 and 4×10^8 M^{-1} s^{-1} for Trp-45. For comparison, NATA, with a fluorescence lifetime of 3.0 ns and a K_{SV} value of 10.5 M^{-1}, has a k_q value of 3.5×10^9 M^{-1} s^{-1}, which is close to that expected for unhindered diffusion. Thus, the quenching results support the absorption and fluorescence spectra and together indicate strongly that Trp-14 and Trp-45 are largely buried and have limited exposure to solvent; Trp-14 is the more buried residue because it has the more blue-shifted emission spectrum and the smaller bimolecular quenching constant (cf. Eftink, 1991).

It is noteworthy that the fluorescence emission intensity of W158F, when measured with 280-nm excitation, is greater than that of sTF, and the resulting difference emission spectrum has a maximum at ~310 nm (Fig. 6). This difference spectrum is characteristic of Tyr, and it suggests that in sTF the fluorescence of one or more nearby Tyr residues are quenched

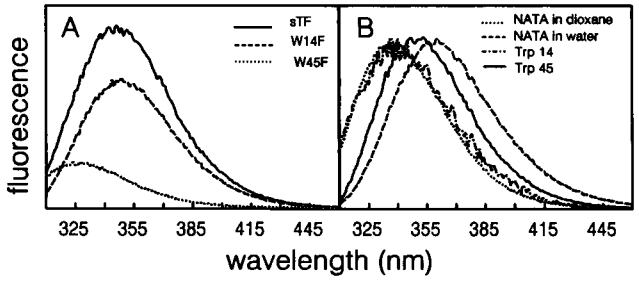

FIGURE 5 Fluorescence emission spectra of sTF (–), W14F (- - -), and W45F (····) at 3 μM. (*B*) Normalized fluorescence emission spectra of Trp-14 (-·-) and Trp-45 (–) as compared with NATA in aqueous buffer (- - -) and dioxane (····).

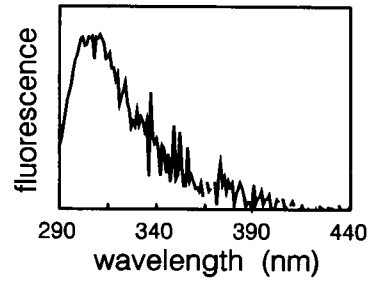

FIGURE 6 Fluorescence difference spectrum between W158F and sTF excited at 280 nm.

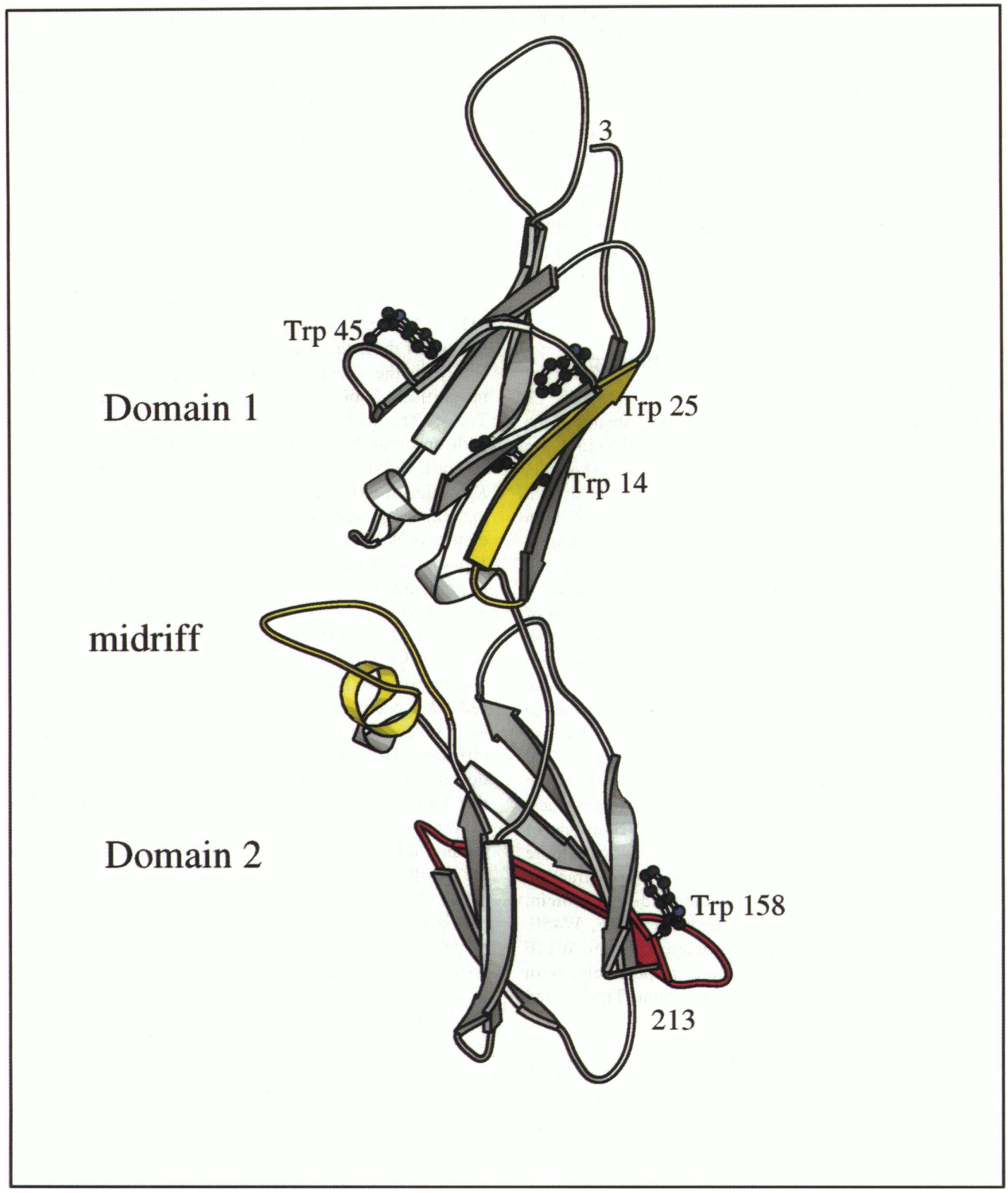

FIGURE 7 MOLSCRIPT (Kraulis, 1991) representation of sTF_{1-219}. The indole side chains of the four Trp residues are shown as ball-and-stick representations. Numbers 3 and 213 indicate the first and last ordered residues in the structure.

by resonance energy transfer to Trp-158. There are three near-neighbor Tyr residues in the primary structure surrounding Trp-158 that could be potential excitation energy donors. It is also possible, however, that the donors could be other Tyr residues that are near Trp-158 as a result of the tertiary structure of the folded protein.

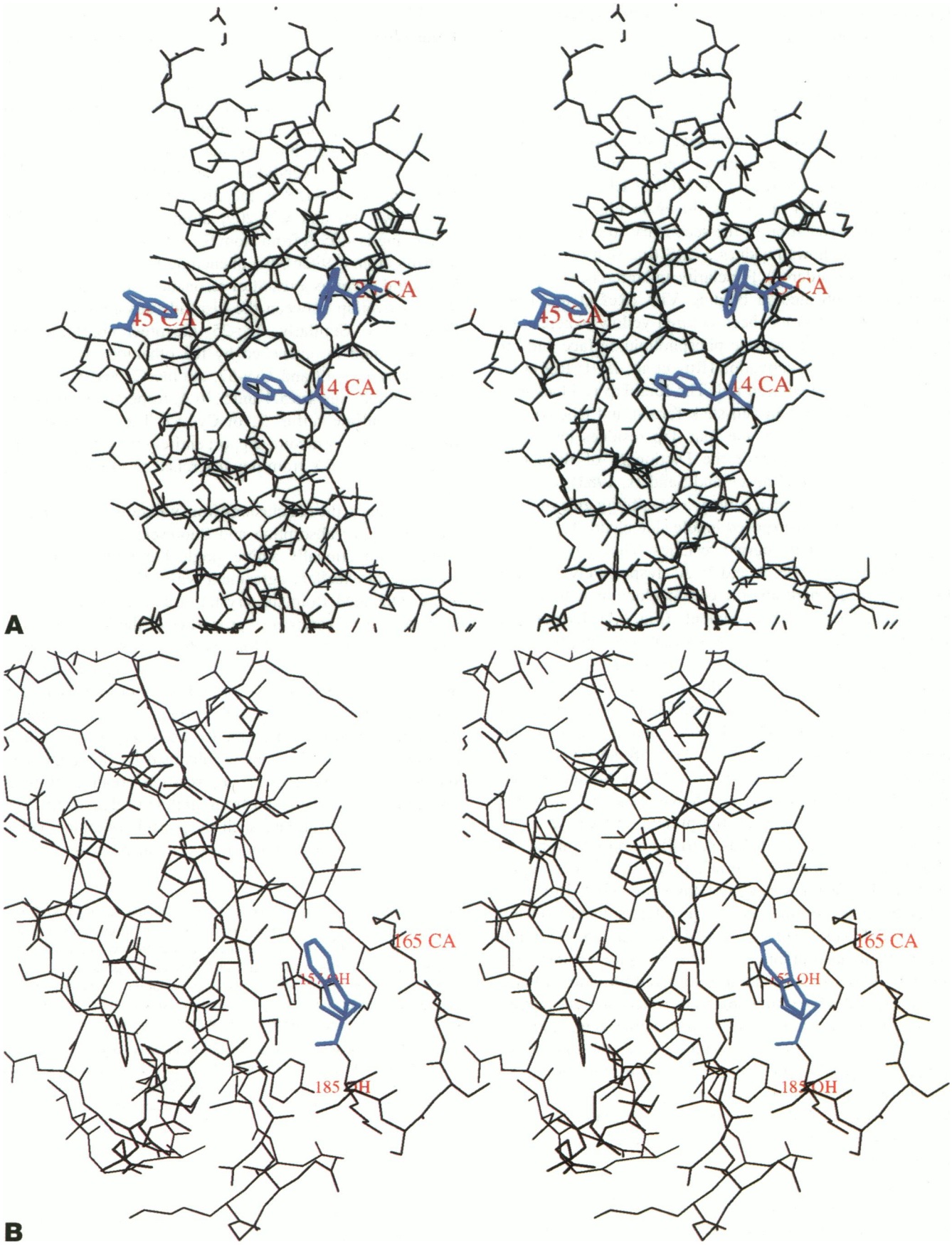

FIGURE 8 Stereo representations of the local environments of the four tryptophan residues in sTF. (*A*) View of domain 1 showing Trp-4, Trp-25, and Trp-45. (*B*) View of domain 2 showing Trp-158.

Evaluation of the spectroscopy results in terms of the crystal structure of sTF

As recently described, the crystal structure of the extracellular region of tissue factor comprising the first 219 residues has now been solved (Harlos et al., 1994; see also Muller et al., 1994). sTF consists of two seven-stranded β-sandwich immunoglobulin-like domains (1 and 2) joined by an extensive novel midriff region. A MOLSCRIPT representation (Kraulis, 1991) of sTF is shown in Fig. 7. This is a graphical representation of the secondary structure in three dimensions. It shows residues 3–213 (the first two and the last six were disordered). For clarity and reference purposes, the region implicated in binding VIIa (Ruf et al., 1994; Muller et al., 1994) has been colored yellow, whereas the region in domain 2 near the phospholipid surface and implicated in factor X activation (Roy et al., 1991; Ruf et al., 1992a,b) has been colored red. The four Trp residues have been highlighted in ball-and-stick format and labeled. The solvent accessibilities of the four Trp residues have been calculated with the use of the Dictionary of Secondary Structure Prediction (Kabsch and Sanders, 1983).

When compared with a solvent accessibility area of 340–350 Å^2 for a solvent-exposed indole side chain, Trp-14 and Trp-25 are essentially buried residues. They have solvent accessibility areas of ~39 and 16 Å^2, respectively, and they form part of the hydrophobic core of domain 1; both residues are in restricted environments (Fig. 8*A*). By contrast, Trp-45 has a significantly larger solvent accessibility area of 86 Å^2 for its indole side chain. According to the fluorescence emission spectra and fluorescence quenching with iodide ion, Trp-14 is more buried than Trp-45, and both residues are largely shielded from solvent, as is evident from the crystal structure model. Trp-158, however, with a solvent-accessible area of 41 Å^2, has a limited solvent exposure, similar to Trp-14. As shown in Fig. 8*B*, the indole ring of Trp-158 is lying on the protein surface but is not projecting into solvent. It lies partially exposed on the end of a strand in domain 2, and it is in the middle of a region implicated in factor X binding (Roy et al., 1991; Ruf et al., 1992a,b). Based on the nearly equivalent solvent exposure of the indole side chains of Trp-14 and Trp-158, one might expect their absorption spectra to be more similar. It is possible, however, that the less resolved vibrational bands of the Trp-158 absorption spectrum reflect solvent interactions with different regions of the indole ring. Tyr-153, Tyr-156, and Tyr-157 are residues close in primary sequence to Trp-158, which might account for the appearance of the additional Tyr emission in the fluorescence of W158F. Any or all of these Tyr residues could be quenched by resonance energy transfer to Trp-158 in sTF. In addition, it should be noted that, as a result of folding in the tertiary structure of sTF, the phenol ring of Tyr-185 is within 10 Å of the indole ring of Trp-158, which is close enough for quenching the fluorescence of this Tyr residue by resonance energy transfer to Trp-158 (see Tyr difference emission spectrum of W158F in Fig. 6). The efficient quenching of Trp-158, making it nonfluorescent, could result from interaction with the ammonium group of Lys-165, which, in the crystal structure, lies 3–5 Å from the face of the indole ring. As shown by Barkley and co-workers (Yu et al., 1992), ammonium groups are efficient quenchers. Lys-165 is part of a flexible loop, and increased mobility could enhance the possibility of quenching by the protonated Lys ε-amino group. A second candidate that could account for the quenching of Trp-158 is the disulfide bridge formed between Cys-186 and Cys-209; atom $C_{\epsilon 2}$ of the Trp-158 indole ring is 4.05 Å from atom S_γ of Cys-186; as discussed by Ross et al. (1992b), the quenching by a proximal disulfide could occur as a result of resonance energy transfer, as there is overlap between the disulfide absorption and Trp fluorescence. Similarly, Trp-25, the other nonfluorescent residue, could be quenched by the other disulfide bridge formed by Cys-49 and Cys-57. Atoms C_η and $C_{\zeta 3}$ of the Trp-25 indole ring are 5.4 and 5.46 Å, respectively, from the nearest disulfide sulfur, S_γ of Cys-57. These observations from the crystal structure support entirely the interpretations of Trp fluorescence from the difference spectroscopic measurements.

In summary, the conclusions from solution measurements with difference absorption and fluorescence spectroscopy, based on functionally active single-Trp replacement mutants, are in excellent agreement with solvent accessibility areas calculated from the crystal structure model of sTF. Moreover, the fluorescence properties of the individual Trp residues can be accounted for readily by the crystal structure model. Thus, in the absence of an x-ray crystal structure model, we anticipate that information about individual Trp environments, even in multi-Trp proteins, can be obtained by similar solution measurements. For example, we anticipate that resolved Trp spectra, obtained by this approach, should provide more direct information about conformational transitions that result from binding of ligands or from reversible modifications, such as phosphorylation, which are important in the regulation of cellular processes.

We thank Drs. Donald Senear, Thomas Laue, Thomas Kumosinski, Harry Andree, William Laws, and David Teller for useful discussions. We also acknowledge Mr. Paul Contino who carried out the development of the automated robotic system and protocols for the chromogenic assay used in this work, and Dr. Mihaly Mezei, who helped with the computer graphics. Dr. Igor Polikarpov acknowledges support by SERC, and Dr. C. William G. Boys acknowledges support by the Wellcome Trust.

This work was supported by U.S. Public Health Service grants HL-29019 and GM-39750. Preliminary accounts of parts of this work were presented at the American Chemical Society Meeting in Denver, CO, in April, 1993, and at the International Society for Optical Engineering Meeting in Los Angeles, CA, in January, 1994.

REFERENCES

Bach, R. 1988. Initiation of coagulation by tissue factor. *CRC Crit. Rev. Biochem.* 23:339–368.

Badea, M. G., and L. Brand. 1979. Time-resolved fluorescence measurements. *Methods Enzymol.* 61:378–425.

Bazan, J. F. 1990. Structural design and molecular evolution of a cytokine receptor superfamily. *Proc. Natl. Acad. Sci. USA.* 87:6934–6938.

Broze, G. J., and P. W. Majerus. 1980. Purification and properties of human coagulation Factor VIII. *J. Biol. Chem.* 255:1242–1247.

Di Scipio, R. G., M. A. Hermodson, S. G. Yates, and E. W. Davie. 1977. A comparison of human prothrombin, factor IX (Christmas factor), factor X (Stuart factor), and protein S. *Biochemistry.* 16:698–705.

Edgington, T. S., N. Mackman, K. Brand, and W. Ruf. 1991. The structural biology of expression and function of tissue factor. *Thromb. Haemost.* 66:67–79.

Eftink, M. R. 1991. Fluorescence techniques for studying protein structure. *Methods Biochem. Anal.* 35:127–205.

Eftink, M. R. 1994. The use of fluorescence methods to monitor unfolding transitions in proteins. *Biophys. J.* 66:482–501.

Fiore, M. M., P. F. Neuenschwander, and J. H. Morrissey. 1994. The biochemical basis for the apparent defect of soluble mutant tissue factor in enhancing the proteolytic activities of factor VIIa. *J. Biol. Chem.* 269:143–149.

Harlos, K., D. M. A. Martin, D. P. O'Brien, E. Y. Jones, D. I. Stuart, I. Polikarpov, A. Miller, E. G. D. Tuddenham, and C. W. G. Boys. 1994. Crystal structure of the extracellular domain of human tissue factor. *Nature.* 370:662–666.

Hasselbacher, C. A., E. Waxman, L. T. Galati, P. B. Contino, J. B. A. Ross, and W. R. Laws. 1991. Investigation of hydrogen bonding and proton transfer of aromatic alcohols in nonaqueous solvents by steady-state and time-resolved fluorescence. *J. Phys. Chem.* 95:2995–3005.

Kabsch, W., and C. Sanders. 1983. Dictionary of protein secondary structure: pattern recognition of hydrogen-bonded and geometrical features. *Biopolymers.* 22:2577–2637.

Kraulis, P. J. 1991. Molscript: a program to produce both detailed and schematic plots of protein structures. *J. Appl. Crystallogr.* 24:946–950.

Lakowicz, J. R. 1983. Principles of Fluorescence Spectroscopy. Plenum Press, New York.

Laws, W. R., and P. B. Contino. 1992. Fluorescence quenching studies: analysis of nonlinear Stern-Volmer data. *Methods Enzymol.* 210: 448–463.

Miletich, J. P., G. J. Broze, and P. W. Majerus. 1981. Purification of human coagulation factors II, IX, and X using sulfated dextran beads. *Methods Enzymol.* 80:221–228.

Muller, Y. A., M. H. Ultsch, R. F. Kelley, and A. M. de Vos. 1994. Structure of the extracellular domain of human tissue factor: location of the factor VIIa binding site. *Biochemistry.* 33:10864–10870.

Nemerson, Y. 1988. Tissue factor and hemostasis. *Blood.* 71:1–8.

Neuenschwander, P. F., and J. H. Morrissey. 1992. Deletion of the membrane anchoring region of tissue factor abolishes autoactivation of factor VII but not cofactor function. *J. Biol. Chem.* 267:14477–14482.

Rehemtulla, A., W. Ruf, D. J. Miles, and T. S. Edgington. 1992. The third Trp-Lys-Ser (WKS) tripeptide motif in tissue factor is associated with a function site. *Biochem. J.* 282:737–740.

Ross, J. B. A., W. R. Laws, K. W. Rousslang, and H. R. Wyssbrod. 1992a. Tyrosine fluorescence from proteins and polypeptides. *In* Topics in Fluorescence Spectroscopy, Vol. 3. J. R. Lakowicz, editor. Plenum Press, New York. 1–63.

Ross, J. B. A., K. W. Rousslang, and A. L. Kwiram. 1980. Optically detected magnetic resonance of tryptophan triplet states in native and urea-denatured proteins and polypeptides. *Biochemistry.* 19:876–883.

Ross, J. B. A., H. R. Wyssbrod, R. A. Porter, G. P. Schwartz, C. A. Michaels, and W. R. Laws. 1992b. Correlation of tryptophan fluorescence intensity decay parameters with ^{1}H NMR-determined rotamer conformations: [tryptophan^2]oxytocin. *Biochemistry.* 31:1585–1594.

Roy, S., P. E. Hass, J. H. Bourell, W. J. Henzel, and G. A. Vehar, 1991. Lysine residues 165 and 166 are essential for the cofactor function of tissue factor. *J. Biol. Chem.* 266:22063–22066.

Ruf, W., and T. S. Edgington. 1991. Two sites in the tissue factor extracellular domain mediate the recognition of the ligand factor VIIa. *Proc. Natl. Acad. Sci. USA.* 88:8430–8434.

Ruf, W., D. J. Miles, A. Rehemtulla, and T. S. Edgington. 1992a. Cofactor residues lysine 165 and 166 are critical for protein-substrate recognition by the tissue-factor-factor-VIIa protease complex. *J. Biol. Chem.* 267: 6375–6381.

Ruf, W., D. J. Miles, A. Rehemtulla, and T. S. Edgington. 1992b. Tissue factor residues 157–167 are required for efficient proteolytic activation of factor X and factor VII. *J. Biol. Chem.* 267:22206–22210.

Ruf, W., J. R. Schullek, M. J. Stone, and T. S. Edgington. 1994. Mutational mapping of functional residues in tissue factor: identification of factor VII recognition determinants in both structural modules of the predicted cytokine receptor homology domain. *Biochemistry.* 33:1565–1572.

Spicer, E. K., R. Horton, L. Bloem, R. Bach, K. R. Williams, A. Guha, J. Kraus, T. C. Lin, Y. Nemerson, and W. H. Konigsberg. 1987. Isolation of cDNA clones coding for human tissue factor: primary structure of the protein and cDNA. *Proc. Natl. Acad. Sci. USA.* 84:5148–5152.

Strickland, E. H., J. Horwitz, E. Kay, L. M. Shannon, M. Wilcheck, and C. Billups. 1971. Near-ultraviolet absorption bands of tryptophan: studies using horseradish peroxidase isoenzymes, bovine and horse heart cytochrome c, and *N*-stearyl-L-tryptophan *n*-hexyl ester. *Biochemistry.* 10: 2631–2638.

Valeur, B., and G. Weber. 1977. Resolution of the fluorescence excitation spectrum of indole into the ^1L_a and ^1L_b excitation bands. *Photochem. Photobiol.* 25:441–444.

Waxman, E., W. R. Laws, T. M. Laue, Y. Nemerson, and J. B. A. Ross. 1993b. Human factor VIIa and its complex with soluble tissue factor: evaluation of assymetry and conformational dynamics by ultracentrifugation and fluorescence anisotropy decay methods. *Biochemistry.* 32: 3005–3012.

Waxman, E., J. B. A. Ross, T. M. Laue, A. Guha, S. V. Thiruvikraman, T. C. Lin, W. H. Konigsberg, and Y. Nemerson. 1992. Tissue factor and its extracellular soluble domain: the relationship between intermolecular association with factor VIIa and enzymatic activity of the complex. *Biochemistry.* 31:3998–4003.

Waxman, E., E. Rusinova, C. A. Hasselbacher, G. P. Schwartz, W. R. Laws, and J. B. A. Ross. 1993a. Determination of the tryptophan: tyrosine ratio in proteins. *Anal. Biochem.* 210:425–428.

Wetlaufer, D. B. 1962. Ultraviolet spectra of proteins and amino acids. *Adv. Protein Chem.* 17:303–390.

Yu, H.-T., W. J. Colucci, M. L. McLaughlin, and M. D. Barkley. 1992. Fluorescence quenching in indoles by excited-state proton transfer. *J. Am. Chem. Soc.* 114:8449–8454.